

Complex Pharmacological Properties of Recombinant α -Amino-3-hydroxy-5-methyl-4-isoxazole Propionate Receptor Subtypes

ELKE STEIN,¹ JANE A. COX,¹ PETER H. SEEBURG, and TODD A. VERDOORN

Department of Pharmacology, Vanderbilt University, Nashville, Tennessee 37232-6600 (E.S., T.A.V.), Max-Planck Institut für Medizinische Forschung, Abteilung Zellphysiologie, D-6900 Heidelberg, Germany (J.A.C.; and Laboratory of Molecular Neuroendocrinology, Center for Molecular Biology (ZMBH), University of Heidelberg, D-6900 Heidelberg, Germany (P.H.S.)

Received July 20, 1992; Accepted August 20, 1992

SUMMARY

The pharmacological properties of two glutamate receptor subtypes, GluR-A/B and GluR-B/D, were examined in RNA-injected *Xenopus* oocytes using two-electrode voltage clamp. Concentration-response relations revealed that the potencies of L-glutamate, kainate, and α -amino-3-hydroxy-5-methyl-4-isoxazole propionate (AMPA) varied slightly between the two receptor subtypes, but the rank order of agonist potency did not. The EC₅₀ values for GluR-A/B receptors were 3.31 μ M for AMPA, 6.16 μ M for glutamate, and 57.5 μ M for kainate, whereas the EC₅₀ values for GluR-B/D receptors were 5.01 μ M, 32.3 μ M, and 64.6 μ M for AMPA, L-glutamate, and kainate, respectively. The potencies of 6-cyano-7-nitroquinoxaline-2,3-dione (CNQX) and 2,3-dihydroxy-6-nitro-7-sulfamoyl-benzo(f)quinoxaline (NBQX) were quantified by Schild analysis. The potency of NBQX at blocking currents mediated by GluR-A/B receptors changed depending on the agonist used to activate the receptors (pA₂ values were as follows: for block of kainate, 7.23 \pm 0.01; L-glutamate, 6.78 \pm

0.02; AMPA, 6.95 \pm 0.02). Differences between agonists were less marked in cells expressing GluR-B/D receptors (pA₂ values: kainate, 7.28 \pm 0.01; L-glutamate, 7.30 \pm 0.02; AMPA, 7.35 \pm 0.01). In each case, the slope of the Schild regression was not different from unity, consistent with competitive antagonism of these receptors by NBQX. CNQX also blocked GluR-A/B and GluR-B/D receptors competitively but was less potent than NBQX and did not differentiate between agonists or subunit combination. These data suggest that L-glutamate, kainate, and AMPA bind to different receptor substructures on recombinant AMPA receptors and that NBQX but not CNQX binds to these sites with different affinities. Moreover, because the properties of these binding sites vary between GluR-A/B and GluR-B/D receptors, our findings provide a basis for mutational analysis aimed at identifying receptor domains involved in agonist and antagonist binding.

The isolation of cDNA clones encoding numerous subunits of neuronal excitatory amino acid receptors has led to a re-evaluation of the hypothesis that only three types of ionotropic glutamate receptors exist (1). The ability of homomeric and heteromeric subunits to form functional glutamate-activated channels and the multiplicity of clones encoding subunits of NMDA (2-5), AMPA (6-11), and kainate receptors (12-16) indicate that heterogeneity may exist within each classical receptor type. At least four subunits, named GluR-A, -B, -C, and -D or GluR-1, -2, -3, and -4, are thought to constitute the AMPA receptor type, and each of these exists in two or more variants generated by alternative splicing (9, 17). The functional properties of AMPA receptors expressed from combinations of one, two, or three different subunits are reminiscent of native receptors, but the constellation of subunits that make

up native receptors is unknown. Moreover, the extent and nature of functional heterogeneity in the brain are unexplored.

One way to clarify the relationship between native and recombinant receptors is to compare their pharmacological properties and determine how cloned receptors fit into the receptor classification system for native receptors. A valuable tool in this endeavor is the quantitative measurement of antagonist potency (18). Based on this criterion, native AMPA receptors are defined as those receptors that have a high affinity for the antagonists CNQX and NBQX (19, 20) and low affinity for the NMDA receptor blocker D-APV (21). The variety of subunits that could potentially constitute AMPA receptors may lead to significant receptor heterogeneity. Thus, multiple AMPA receptor subtypes may exist, each having different affinities for CNQX, NBQX, or other compounds. It is, therefore, important to determine the degree of pharmacological diversity that arises from recombinant AMPA receptor subunits.

This work was supported in part by a Pharmaceutical Manufacturers Association Foundation Research Starter Award (T.A.V.).

¹ The first two authors contributed equally to this report.

ABBREVIATIONS: NMDA, N-methyl-D-aspartate; AMPA, α -amino-3-hydroxy-5-methyl-4-isoxazole propionate; CNQX, 6-cyano-7-nitroquinoxaline-2,3-dione; NBQX, 2,3-dihydroxy-6-nitro-7-sulfamoylbenzo(f)quinoxaline; D-APV, D-amino-5-phosphonoveralate; HEPES, N-[2-hydroxyethyl]piperazine-N'-[2-ethanesulfonic acid].

We have expressed different combinations of AMPA receptor subunits in *Xenopus* oocytes and determined the potencies of the agonists L-glutamate, AMPA, and kainate and the antagonists NBQX and CNQX. This expression system is well suited for quantitative pharmacological studies, and the expression of cloned receptors offers the significant advantage of allowing the examination of a single receptor type in isolation. Our results indicate that NBQX shows selectivity for different subunit combinations and for currents activated by different agonists within one subunit combination. These data suggest that L-glutamate, kainate, and AMPA may bind to different sites on a single structural entity.

Materials and Methods

RNA preparation. DNA sequences encoding the flip forms of GluR-A, -B, and -D were subcloned from the original expression constructs (7, 9) into the *Xenopus* oocyte expression vector pSP64T (22). For transcription of RNA, plasmids were linearized with the restriction enzyme *SalI* (Boehringer Mannheim) and cRNA containing 5'-7-MeGpppG cap analogue (Pharmacia) was synthesized using SP6 RNA polymerase (Promega), according to the method of Krieg and Melton (22). The DNA template was removed by digestion with RNase-free DNase I (Boehringer Mannheim) followed by treatment with proteinase K (Boehringer Mannheim). The RNA was extracted twice with phenol, twice with phenol/chloroform (1:1), and twice with chloroform, precipitated twice with 0.3 M sodium acetate and 2.5 volumes of 100% ethanol, and stored at -20° in 70% ethanol. Just before injection, the RNA was washed twice with 70% ethanol, dried, and resuspended in diethylpyrocarbonate-treated water at a final concentration of 0.5 $\mu\text{g}/\mu\text{l}$. RNA dissolved in water was sometimes refrozen and stored at -70° for use in subsequent injections.

Oocyte isolation, injection, and culture. Single *Xenopus laevis* oocytes were removed by manual dissection from isolated ovaries and stored in sterile oocyte Ringer solution consisting of (in mM) 82.5 NaCl, 2.5 KCl, 1.0 CaCl_2 , 1.0 MgCl_2 , 1.0 Na_2HPO_4 , and 5 HEPES, with 0.5 g/liter polyvinylpyrrolidone, 25, pH 7.2. Oocytes were then injected with 25–50 ng of RNA using borosilicate pipets with a tip diameter of 5–10 μm . For expression of heteromeric combinations a 1:2 (w/w) ratio of GluR-A or GluR-D to GluR-B cRNA was injected. After injection, oocytes were maintained in oocyte Ringer solution containing penicillin/streptomycin (100 units/ml each) and zinacef (0.4 mg/ml), in 96-well tissue culture plates (Falcon 3072), at 19° . Twenty-four hours after injection, the oocytes were treated with collagenase (type II, 1 mg/ml; Sigma, St. Louis, MO) for 1 hr at room temperature. After three washes with oocyte Ringer solution, the follicle cell layer was manually removed with fine forceps. The oocytes were then placed in fresh Ringer solution and maintained at 19° until used for experiments (3–4 days after injection).

Electrophysiology. Oocytes were voltage clamped at -50 to -70 mV with two microelectrodes filled with 3 M KCl or 3 M CsCl and were continuously perfused with frog Ringer solution (115 mM NaCl, 2.5 mM KCl, 1.8 mM CaCl_2 , 10 mM HEPES, pH 7.2, 240 mOsm). Agonists and antagonists were dissolved in frog Ringer solution and applied by gravity perfusion. Perfusion of agonists continued until a steady response was obtained (about 30 sec), whereas blockers (CNQX, NBQX, or L-glutamate) were applied for 3 min before challenge with agonist to allow for complete equilibration with the receptors. Currents were filtered at 20 Hz (-3 dB, eight-pole Bessel; Frequency Devices) and recorded either on a chart recorder or directly on-line using a Macintosh-IIx computer and an Instrutech ITC-16 A-D interface.

Agonist concentration-response curves were constructed by measuring the maximum current induced by increasing concentrations of agonist. Data from individual cells were fitted to the logistic equation:

$$I = I_{\max}/1 + ([\text{agonist}]/\text{EC}_{50})^{n^H} \quad (1)$$

where I is the steady state current produced by [agonist]. The parameters I_{\max} (maximum current at infinite [agonist]), n^H (the Hill coefficient), and EC_{50} (concentration of agonist producing 50% of I_{\max}) were determined by an iterative least squares fitting routine. Means, standard errors, and 95% confidence intervals were calculated using the logarithm of individual EC_{50} estimates. The IC_{50} values for glutamate were determined by fitting the data to eq. 1, except that EC_{50} was replaced with IC_{50} and n^H was negative. Schild analyses were performed essentially as described (21). Briefly, three concentrations of agonist were applied under control conditions, followed by three concentrations (21) in the presence of a given concentration of antagonist. The ratio of equieffective agonist concentrations (dose ratio) was determined by interpolation of a linear regression of current amplitude versus the logarithm of the agonist concentration. One to four antagonist concentrations were tested on each cell. The dose ratios determined from all cells within a particular experimental group were pooled and linear regression of $\log(\text{dose ratio} - 1)$ versus $\log[\text{antagonist}]$ was performed to estimate the slope and the x-axis intercept (pA_2). If the regression was linear and the slope was not significantly different from unity (by analysis of covariance), individual pA_2 values were estimated from each dose ratio (DR) using the following variant of the Schild equation:

$$\text{pA}_2 = \log[\text{antagonist}] - \log(\text{DR} - 1) \quad (2)$$

For this analysis to be valid the pA_2 values must be independent of $\log[\text{antagonist}]$. Linear regression of this relationship performed on each data set showed no correlation between these pA_2 values and $\log[\text{antagonist}]$ (see Fig. 4D). This method of analysis allows all dose ratio measurements to contribute equally to the mean value, regardless of the number of observations made on particular oocytes. The mean pA_2 values and standard errors reported in Tables 2 and 3 were derived in this manner. Differences between experimental groups were analyzed by Students t test or analysis of covariance.

Current-voltage (I - V) curves were constructed by ramping the membrane potential from 0 mV to +60 mV and then down again to -60 mV over 4 sec. Currents measured at rest were digitally subtracted from those measured in the presence of agonist, to produce agonist-activated I - V curves. Digitized data points were averaged over 3 mV and the averaged points were fitted to third- to fifth-order polynomial functions that were used to calculate the reversal potentials and conductances at particular membrane potentials.

AMPA and CNQX were obtained from Tocris Neuramin and all other reagents were from Sigma. NBQX was obtained from Dr. Tage Honore of Novo Nordisk and Dr. Jorgen Drejer of NeuroSearch.

Results

Oocytes expressing homomeric GluR-A(flip) or GluR-D(flip) or heteromeric combinations of GluR-A(flip) and -B(flip) (termed GluR-A/B) or GluR-B/D responded robustly to applications of L-glutamate, AMPA, or kainate within 3 days after RNA injection. The average maximum currents (I_{\max} from eq. 1) induced by L-glutamate, AMPA, and kainate in cells expressing GluR-A/B receptors were 370 ± 175 ($n = 12$), 826 ± 365 ($n = 10$), and 1274 ± 299 nA ($n = 18$), respectively. For GluR-B/D receptors average maximum currents were 1216 ± 350 ($n = 8$), 833 ± 274 ($n = 11$), and 1855 ± 490 nA ($n = 9$) for L-glutamate, AMPA, and kainate, respectively. As observed by others (8, 10), oocytes expressing homomeric GluR-B receptors responded poorly to the agonists used here and were not characterized further. The currents observed in oocytes represent the steady state component of agonist responses. The desensitizing peak current evoked by L-glutamate and AMPA upon rapid agonist application was not seen because of slow solution changes around large-diameter oocytes. The flip variants were used so that steady state currents evoked by L-glutamate and AMPA could be observed more readily. Expression of flop

variants results in markedly smaller steady state L-glutamate and AMPA currents in both oocytes (6, 8, 23) and transfected fibroblasts (9), due to rapid and extensive inactivation.

The relative potencies of L-glutamate, AMPA, and kainate were estimated from the concentration-response relationship of the steady state currents (Figs. 1 and 2; Table 1). The

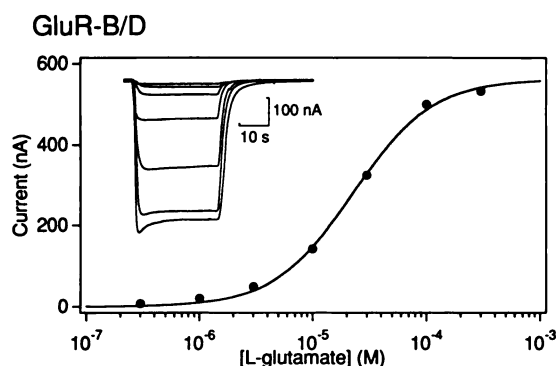
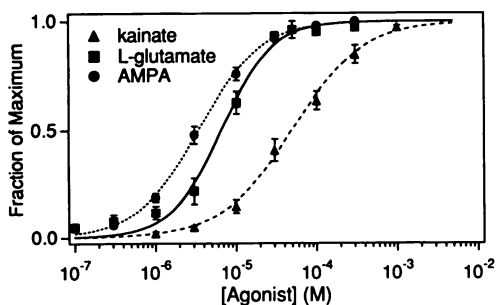


Fig. 1. Example of an L-glutamate concentration-response relationship measured in a *Xenopus* oocyte injected with GluR-B and GluR-D cRNAs. *Inset*, inward currents evoked by 0.3, 1.0, 3.0, 10, 30, 100, and 300 μM L-glutamate. The graph shows the amplitude of the steady state currents measured at the end of the application plotted as a function of [L-glutamate] (logarithmic scale). The smooth curve represents the least squares fit of this data set to eq. 1 (see Materials and Methods). The parameters estimated from these data were $I_{\text{max}} = 562$ nA, $\text{EC}_{50} = 22.8$ μM , and $n_H = 1.26$.

A. GluR-A/B



B. GluR-B/D

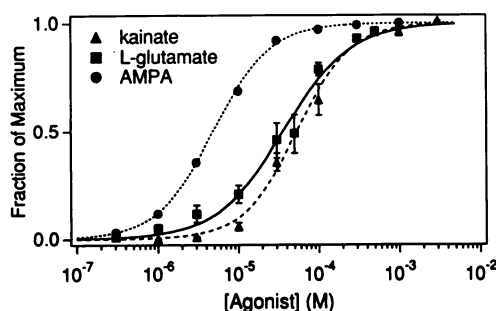


Fig. 2. Agonist potency differs between GluR-A/B and GluR-B/D receptor subtypes. Average concentration-response curves constructed in oocytes expressing GluR-A/B (A) and GluR-B/D (B) are shown. Steady state currents elicited by at least seven concentrations of AMPA, L-glutamate, or kainate were measured. The points represent the mean \pm standard error of the fraction of I_{max} (estimated from individual experiments such as shown in Fig. 2) for between eight and 18 different oocytes. The lines are the least squares fit of the mean points to a variant of the logistic equation: $I/I_{\text{max}} = 1 / (1 + ([\text{agonist}]/\text{EC}_{50})^n)$. The mean EC_{50} values and Hill coefficients are reported in Table 1.

TABLE 1

Agonist pharmacology of recombinant AMPA receptors

The average EC_{50} values and Hill coefficients shown here were derived from the means of individual cells, as described in Materials and Methods. The 95% confidence intervals are shown in parentheses. n is the number of individual cells tested.

Subtype	Kainate	L-Glutamate	AMPA
GluR-A/B			
EC_{50} (μM)	57.5 (48.9–67.6)	6.16 (5.25–7.24)	3.31 (2.95–3.71)
Hill coefficient	1.27 ± 0.05	1.70 ± 0.26	1.21 ± 0.04
n	18	12	10
GluR-B/D			
EC_{50}	64.6 (51.9–80.4)	32.3 (25.7–40.7)	5.01 (4.26–6.11)
Hill coefficient	1.47 ± 0.04	1.30 ± 0.08	1.36 ± 0.04
n	9	8	11

potencies of AMPA and kainate differed only slightly between subunit combinations, whereas L-glutamate was markedly more potent at GluR-A/B receptors than at GluR-B/D receptors (Table 1). The rank order of agonist potency (AMPA > L-glutamate > kainate) did not differ between GluR-A/B and GluR-B/D and appeared to be similar to that found by others studying receptors composed of these subunits (10, 11). In each case the estimated Hill coefficient was greater than unity. Although these findings may indicate that more than one agonist molecule must bind before the receptors is activated, mechanistic interpretations based on the Hill coefficient are problematic because a desensitized state of the receptor is being measured.

AMPA receptor agonists are known to inhibit the actions of one another in neurons (24–30) and in cells expressing cloned subunits (7, 23). We examined the interactions between agonists by measuring the effect of increasing concentrations of L-glutamate on currents evoked by EC_{50} concentrations of AMPA or kainate. The inhibition curves for L-glutamate are shown in Fig. 3. For both GluR-A/B and GluR-B/D receptors L-glutamate was noticeably more potent at blocking AMPA-induced currents than those evoked by kainate. The IC_{50} values (mean and 95% confidence interval) for L-glutamate block of AMPA and kainate currents were 7.41 (6.76–8.13) μM and 66.1 (60.2–72.4) μM , respectively, for GluR-A/B and 15.1 (13.2–17.4) μM and 126 (102–155) μM for GluR-B/D ($n = 4$ for all experimental groups). These observations may result from the different desensitization properties of currents evoked by each agonist. However, another possible explanation is that AMPA, kainate, and L-glutamate have different binding pockets within the substructure of a single structural entity.

We also have measured the potency of CNQX and NBQX at blocking agonist currents in oocytes expressing different subunit combinations. Schild analysis was used to confirm the competitive nature of the block and to detect signs of receptor heterogeneity (18). NBQX and CNQX shifted agonist concentration-response curves to the right in a parallel fashion, and linear Schild regressions with slopes of unity were observed for L-glutamate, AMPA, and kainate currents mediated by GluR-A/B and GluR-B/D receptors (Figs. 4 and 5). Interestingly, in cells expressing GluR-A/B the agonist used to activate the receptors had a large effect on the measured potency of NBQX. A qualitatively similar difference was observed in cells expressing GluR-B/D, but it was much smaller in magnitude. Thus, the potency of NBQX differed between GluR-A/B and GluR-B/D receptors when AMPA or L-glutamate was the agonist but not when kainate activated the receptors. Receptors are rou-

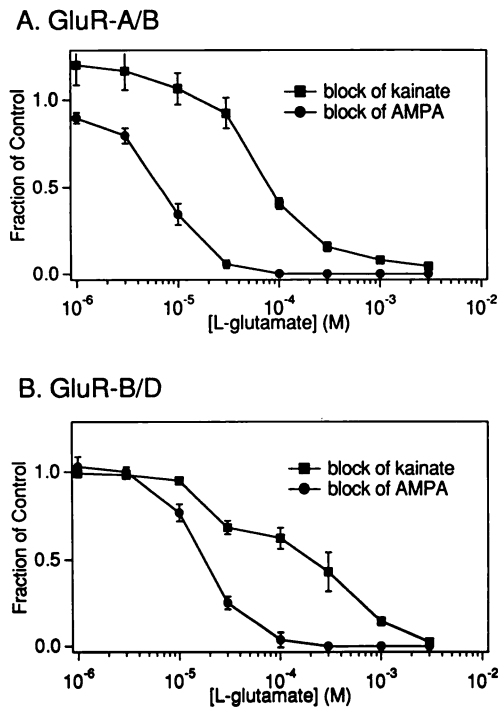


Fig. 3. L-glutamate inhibits kainate- and AMPA-evoked currents with different apparent IC_{50} values. EC_{50} concentrations of kainate (■) or AMPA (●) were applied in the presence of increasing concentrations of L-glutamate. The amplitude of the resulting current was measured after subtraction of the current evoked by L-glutamate alone. The points represent the response amplitude expressed as a fraction of the current evoked by AMPA or kainate alone (means \pm standard errors for four separate experiments), and the lines simply connect the points. **A.** Results of experiments using oocytes expressing GluR-A/B receptors. The average amplitude of current evoked by 3 μ M AMPA in the absence of L-glutamate was 184 ± 29 nA ($n = 4$) and the maximum L-glutamate-evoked current in these cells was 237 ± 36 nA. In the kainate-block experiment the control kainate response (60 μ M kainate) was 300 ± 74 nA and the L-glutamate maximum was 124 ± 24 nA ($n = 4$). At low concentrations of L-glutamate the apparent potentiation of kainate currents was not statistically significant ($p > 0.1$). **B.** Results for GluR-B/D receptors. The mean current evoked by 5 μ M AMPA was 496 ± 224 nA and L-glutamate gave a maximum response of 637 ± 260 nA ($n = 4$). The average current evoked by 60 μ M kainate in the other set of cells was 459 ± 105 nA, whereas the maximum L-glutamate current was 340 ± 65 nA.

tinely defined and classified according to the potency of competitive antagonists. Therefore, the differences in NBQX potency between GluR-A/B and GluR-B/D indicate that these two AMPA receptor isoforms are pharmacologically different receptor types, and the agonist dependence of NBQX potency supports the view that AMPA, kainate, and L-glutamate bind to different structural parts of the receptor.

Alternatively, AMPA, kainate, and L-glutamate may bind to the same site but induce different conformational changes in the receptor. These conformational changes would have to be different for GluR-A/B receptors, compared with GluR-B/D receptors, and only NBQX would be able to perceive this conformational change, because the differences between agonists were much smaller when CNQX was tested (Tables 2 and 3). CNQX also did not differentiate between subunit combinations as well as did NBQX and was generally less potent (Table 3). Thus, it appears that, not only is NBQX more potent than CNQX and more selective for AMPA versus kainate and

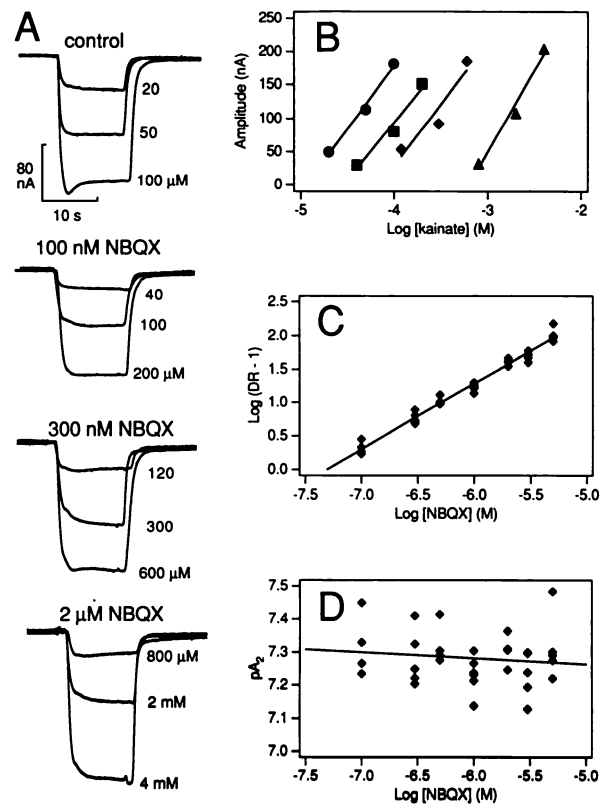
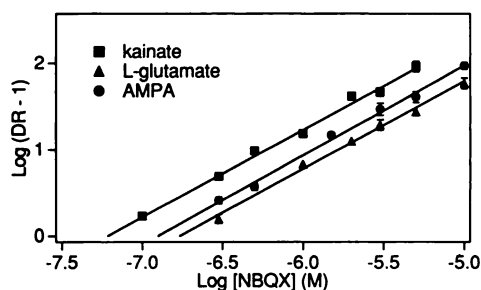


Fig. 4. NBQX competitively blocks recombinant heteromeric AMPA receptors. **A.** Inward currents activated by kainate recorded from an oocyte expressing the GluR-B/D subtype. Control traces are shown at the top, followed by currents measured in the presence of NBQX. The shape of the responses were not qualitatively altered by NBQX. **B.** The parallel shift in the concentration-response relation caused by NBQX in this cell is shown. The points represent the measured amplitude of the currents shown in **A** plotted as a function of log [kainate] under control conditions (●) and in the presence of 100 nM (■), 300 nM (◆), and 2 μ M NBQX (▲). The lines represent linear regressions of these data sets and were used to calculate the dose ratios for Schild analysis. **C.** The logarithms of the dose ratios -1 ($DR - 1$) are plotted as a function of log [NBQX] for the Schild analysis of kainate-evoked currents mediated by GluR-B/D receptors. The points represent the individual dose ratios determined from all cells tested. The line is the result of linear regression of the pooled data points. As summarized in Table 1, the slope of the regression is about 1. **D.** The pA_2 values estimated from each dose ratio according to eq. 2 (see Materials and Methods) are plotted as a function of log [NBQX], showing that there is no relationship between the two parameters, thus validating the method used to estimate the mean pA_2 values from the data. The line is the result of a linear regression of these data. The correlation coefficient was -0.13 .

NMDA receptors (31), it is also potentially more selective for particular AMPA receptor subtypes.

Pharmacological heterogeneity may also arise from expression of multiple structures in these cRNA-injected oocytes. To test this we measured the shape of the $I-V$ curve and the permeability of divalent cations to determine the level of "spare" homomeric GluR-A receptors that are expressed upon injection of a 1:2 ratio of GluR-A and GluR-B RNAs. GluR-A receptors showed marked inward rectification [ratio of chord conductances at +50 mV and -50 mV for kainate-evoked currents, $G(+50)/G(-50) = 0.043 \pm 0.016$; $n = 5$] and permeability to Ba^{2+} (Fig. 6A). Oocytes expressing GluR-A/B receptors gave currents with outward rectification [$G(+50)/G(-50) = 1.34 \pm 0.05$; $n = 21$] and almost no permeability to Ba^{2+} (Fig. 6B). Thus, it seems that the majority of expressed subunits

A. GluR-A/B



B. GluR-B/D

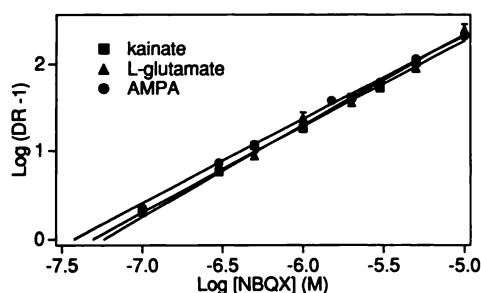


Fig. 5. NBQX interacts differently with two AMPA receptor isoforms. **A**, Schild regressions performed on oocytes expressing GluR-A/B with kainate, AMPA, and L-glutamate used as agonists. The *points* are the means \pm standard errors of dose ratios (*DR*) from all experiments, and the *lines* represent the results of linear regression over each pooled data set. **B**, Results of similar experiments done using oocytes expressing GluR-B/D receptors. Note that each agonist gives a different pA_2 value (*x*-axis intercept) with GluR-A/B but not with GluR-B/D.

TABLE 2

Potency of CNQX at recombinant AMPA receptors

This table summarizes the results of the Schild analyses using CNQX and the agonists listed. The pA_2 values (means \pm standard errors) and slopes (means \pm standard errors) were calculated as described in Materials and Methods. The K_B values were calculated as the negative logarithm of the pA_2 . Number of oocytes represents the number of different oocytes tested and number of observations represents the number of dose ratios that were used for the regression analysis.

Subtype	Kainate	L-Glutamate	AMPA
GluR-A/B			
pA_2	6.35 ± 0.02^a	6.23 ± 0.02^{ab}	6.36 ± 0.04
Slope	1.01 ± 0.04	1.02 ± 0.04	1.05 ± 0.06
K_B (nM)	446	589	437
Number of oocytes	12	12	7
Number of observations	36	35	20
GluR-B/D			
pA_2	6.42 ± 0.02	6.30 ± 0.03^b	6.43 ± 0.01
Slope	1.00 ± 0.04	1.03 ± 0.03	0.99 ± 0.02
K_B (nM)	380	501	372
Number of oocytes	11	8	6
Number of observations	31	23	16

^a Significantly different from GluR-B/D tested with the same agonist ($p < 0.05$).

^b Significantly different from the other agonists tested with the same subunit combination ($p < 0.01$).

assemble into heteromeric combinations containing GluR-B. These data are slightly different from those reported earlier (31, 32), in which an approximately 10-fold excess of GluR-B cRNA was needed to prevent the expression of divalent-permeable, inwardly rectifying receptors.

To examine further the possibility that the observed binding site heterogeneity resulted from assembly of multiple GluR-B-containing heteromers, we repeated the Schild analyses using homomeric GluR-A and GluR-D receptors. Here different

TABLE 3

Potency of NBQX at recombinant AMPA receptors

This table summarizes the results of the Schild analyses using NBQX and the agonists listed. The pA_2 values (means \pm standard errors) and slopes (means \pm standard errors) were calculated from the results of linear regression analysis of data pooled from all oocytes tested. The K_B values were calculated as the negative logarithm of the pA_2 . Number of oocytes represents the number of different oocytes tested and number of observations represents the number of dose ratios that were used for the regression analysis.

Subtype	Kainate	L-Glutamate	AMPA
GluR-A/B			
pA_2	7.23 ± 0.01^{ab}	6.78 ± 0.02^{ac}	6.95 ± 0.02^{ac}
Slope	1.01 ± 0.03	1.02 ± 0.04	1.03 ± 0.03
K_B (nM)	58.8	166	112
Number of oocytes	11	11	8
Number of observations	26	37	24
GluR-B/D			
pA_2	7.28 ± 0.01^a	7.30 ± 0.02	7.35 ± 0.01^a
Slope	0.98 ± 0.03	1.04 ± 0.03	0.96 ± 0.02
K_B (nM)	52.5	50.1	44.6
Number of oocytes	15	12	8
Number of observations	40	33	24
GluR-A			
pA_2	6.86 ± 0.01	6.41 ± 0.02	6.89 ± 0.06
Slope	0.89 ± 0.06^d	0.98 ± 0.03	1.19 ± 0.08^d
K_B (nM)	NC ^e	389	NC
Number of oocytes	8	11	4
Number of observations	24	33	12
GluR-D			
pA_2	7.14 ± 0.02^a	6.99 ± 0.02	7.04 ± 0.03
Slope	0.96 ± 0.03	1.03 ± 0.03	0.94 ± 0.06
K_B (nM)	72.4	102	91.2
Number of oocytes	8	13	4
Number of observations	24	38	12

^a Significantly different from the other agonists tested with the same subunit combination ($p < 0.02$).

^b Significantly different from GluR-B/D tested with the same agonist ($p < 0.05$).

^c Significantly different from GluR-B/D tested with the same agonist ($p < 0.01$).

^d Significantly different from 1.0 ($p < 0.05$).

^e NC, not calculated because slope was not 1.

structures could arise only through assemblies containing different total numbers of subunits. For some agonists, the slopes of the Schild regressions were different from unity (Table 3), preventing rigorous statistical comparisons of antagonist potency, but the pA_2 values showed similar agonist dependence for both GluR-A and GluR-D. It is clear that NBQX blocks currents evoked by different agonists in different ways even when only one subunit is expressed. This strongly suggests that the complex pharmacological properties of recombinant AMPA receptors arise from the structural features of individual subunits and are not the result of multiple subunit assemblies.

Discussion

The pharmacological characterization of cloned receptor subtypes is an important step in determining their identity and their relationship to native receptors, because receptors are most readily defined according to pharmacological criteria. The availability of recombinant receptors allows the expression of single structural entities in isolation and, therefore, greatly facilitates the study of ligand and receptor structure-function relationships. The results reported here show that pharmacological heterogeneity can arise in such a "simplified" model system. Although it is known that CNQX and NBQX differentiate between kainate- and AMPA-mediated responses and [³H]kainate and [³H]AMPA binding sites in neuronal systems (20, 33), such behavior has always been ascribed to the presence of separate AMPA and kainate receptors. Our results can be

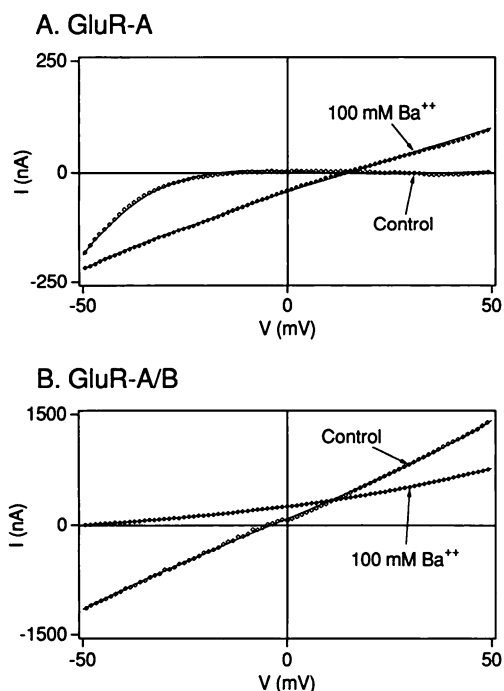


Fig. 6. Ionic permeability of recombinant AMPA receptors. **A**, Ramp *I-V* curves of kainate-activated currents constructed under control conditions and after the replacement of the extracellular Na⁺ and K⁺ with 100 mM Ba²⁺. Currents were recorded in an oocyte expressing GluR-A receptors. The points represent the raw data; the lines are the result of fitting the data to third- or fifth-order polynomial equations. **B**, An identical experiment performed with an oocyte expressing GluR-A/B receptors. Note that the control *I-V* curves in the two cells have different shapes and the reversal potential for Ba²⁺ is markedly more negative in this cell than in the cell expressing GluR-A.

best explained if there exist separate binding sites for each agonist within the substructure of the subunits forming the receptor. These binding sites are likely to be physically close or overlapping, because the agonists block the actions of each other. NBQX block of GluR-A/B receptors clearly demonstrates the different pharmacology of each agonist binding site, but the differences between agonists are smaller when GluR-B/D receptors are used. Because L-glutamate blocks kainate and AMPA currents with different IC₅₀ values in both receptor types, separate agonist binding sites probably exist in GluR-B/D as well, but NBQX does not strongly distinguish between them.

An alternative explanation for our observations would be that each agonist induces a different conformational change in the receptor, imparts different desensitization properties, or even binds to the receptors with different stoichiometry. Our results cannot entirely rule out these possibilities, but we believe such explanations to be less likely. Only NBQX would be able to recognize differences in the effect of agonists and they would have to be less prominent in GluR-B/D than in GluR-A/B receptors. However, native (34, 35) and recombinant (9) AMPA receptors show markedly different responses to L-glutamate, AMPA, and kainate. AMPA and L-glutamate induce rapidly desensitizing currents, whereas kainate currents show no desensitization. In cultured hippocampal neurons the extent of desensitization was shown to vary between a number of agonists (34). AMPA and kainate also activate channels with different conductance states in cells expressing GluR-A to -D subunits (36). Such observations support the contention that

different agonists cause different conformational changes in the receptor molecule. One attractive speculation is that the type of conformational change caused by a particular agonist depends upon the site within the receptor substructure to which the agonist binds.

If differences in agonist desensitization properties underlie the observed differences in NBQX potency, then NBQX should affect desensitization properties as well as block the agonist binding site. This effect on desensitization would be less prominent for CNQX. We are currently testing this hypothesis using rapid agonist application techniques. If multiple agonist binding sites underlie our observations, then point mutations in the ligand binding domain would be expected to affect the affinity of various agonists differently. This hypothesis will also be tested.

The data presented here do not support the alternative hypothesis that multiple receptor structures are assembled and expressed upon injection of RNA encoding two different subunits. The shape of the *I-V* curve and the divalent permeability of heteromeric GluR-A/B receptors indicate that few if any homomeric GluR-A receptors contribute to the agonist responses. Differences in the effect of NBQX were also observed when homomeric GluR-A or GluR-D receptors were tested. Moreover, if different kainate-, AMPA-, or L-glutamate-preferring structures are expressed, each agonist must be completely selective for its particular isoform in order to produce linear Schild regressions with slopes of 1. For example, if L-glutamate activated both the L-glutamate-preferring isoform (for which NBQX has a lower affinity) and the kainate-preferring isoform (for which NBQX has a higher affinity), either there would be a noticeable nonlinearity in the Schild regression or the overall slope would be less than 1. This was clearly not the case.

Our observations are in harmony with previous work that examined the interactions between agonists acting on neuronal AMPA or kainate receptors (24–30). Mutual inhibition of agonist responses has been demonstrated in a number of preparations. The properties of this inhibition were either competitive or noncompetitive, leading to conflicting conclusions about the number of different receptors being studied. Previous work (9) and the observations reported here clearly demonstrate that kainate, AMPA, and L-glutamate act on the same receptor structure, a conclusion also reached by Patneau and Mayer (30) for native AMPA receptors expressed in hippocampal neurons. The noncompetitive interactions previously observed could also be a property arising from a single class of AMPA receptors, because the binding sites for different agonists may physically overlap to various degrees in different receptor subtypes.

NBQX not only distinguished between agonist binding sites but also differentiated between subunit combination. NBQX showed a slightly higher affinity for GluR-B/D versus GluR-A/B when kainate was the agonist and more marked differences when L-glutamate and AMPA were used. Such differences eventually could be exploited for structure-function studies designed to identify receptor substructures responsible for agonist and antagonist binding. The potency differences seem to be conferred by GluR-A and/or GluR-D, and it is anticipated that construction of chimeric subunits containing shuffled domains of GluR-A and GluR-D will likely reveal which structural features of these subunits confer these differences in antagonist potency. The present findings also suggest that it may be possible to design and develop drugs that selectively target

subpopulations of AMPA receptors composed of different subunit combinations. More detailed knowledge of the subunit stoichiometry and structural heterogeneity of native AMPA receptors would facilitate such an effort.

Another goal of these studies was to make comparisons between native and recombinant AMPA receptors. GluR-A/B and GluR-B/D receptors were chosen because these subunit combinations may be constituents of different AMPA receptor isoforms showing differential distribution in the brain. *In situ* hybridization studies have shown that the flip form of GluR-B is widely distributed throughout the central nervous system, and it seems likely that GluR-B is an important constituent of many neuronal AMPA receptors (9). However, GluR-A and GluR-D are expressed in separate brain regions (7, 9, 37). GluR-A flip is found throughout the nervous system, particularly in the hippocampus, the cortex, and cerebellar Purkinje cells. The expression of GluR-D flip mRNA appears to be confined to the cerebellum. Besides the flip and flop splice variants GluR-D also shows variable carboxyl-terminal regions that appear to arise from alternative splicing (17). Although these splice variants are expressed in different cell populations, no clear functional differences associated with this alternative splicing event have yet been demonstrated. We used the flip form of each mainly because currents evoked by glutamate and AMPA show prominent steady state components that can be measured in *Xenopus* oocytes. The effect of the alternative splice module on the pharmacology of the resulting receptors was not tested here, but the pharmacology of the [³H]AMPA binding site is unaffected by this switch (9).

The pharmacological properties of these recombinant subunits are similar but not identical to those of AMPA receptors tested in native neurons (30, 34, 38, 39) and brain mRNA-injected *Xenopus* oocytes (21, 40, 41). The agonists tended to be slightly more potent at activating recombinant receptors than native receptors, but the rank order of agonist potency was the same (AMPA > L-glutamate > kainate). Similar observations have been reported for homomeric GluR-A(flop) (23). Interestingly, Randle *et al.* (41) have reported NBQX potency differences between agonists in brain mRNA-injected *Xenopus* oocytes that closely parallel those we have observed. The receptors expressed in dorsal root ganglion neurons show a different rank order of potency (kainate > L-glutamate > AMPA) (42). Receptors expressed from GluR-5 (16) and GluR-6 (14) subunits show the same order of agonist potency as seen in dorsal root ganglion neurons and an affinity for CNQX that is much lower than that of receptors formed from GluR-A to -D subunits. It seems that GluR-5 and GluR-6 not only are structurally dissimilar but also form a separate pharmacological class.

The potency of CNQX appears to be slightly lower in recombinant receptors than in native receptors (K_B of ~450 nM versus 300 nM for native receptors). NBQX is more potent at blocking recombinant receptors (K_B = 40–102 nM) except for block of L-glutamate responses in GluR-A/B receptors, which gives a K_B of 150 nM, nearly identical to that found for native receptors (33). On the surface, these results suggest that the subunit combinations tested here are not the same as those expressed in neurons. However, direct comparisons between neuronal and recombinant data may be problematic because of the likelihood that measurements in most neuronal preparations arise from multiple subunit structures. As we learn more about the subunit

structure of native receptors, functional comparisons between them will become more meaningful. Moreover, design of experiments in neuronal systems can be guided by the results obtained from characterization of recombinant receptors. For example, the results reported here can be used immediately to guide the discovery and testing of new antagonists that may be more selective for particular AMPA receptor subtypes.

Acknowledgments

We thank Drs. Tage Honore and Jorgen Drejer for the gift of NBQX, Dr. Ralf Schoepfer for constructing some of the plasmids used in initial experiments, Dr. Bert Sakmann for support and advice, and Drs. David Colquhoun, Lee Limbird, and David Lovinger for helpful discussions.

References

1. Watkins, J. C., and R. H. Evans. Excitatory amino acid transmitters. *Annu. Rev. Pharmacol. Toxicol.* 21:165–204 (1981).
2. Moriyoshi, K., M. Masu, T. Ishii, R. Shigemoto, N. Mizuno, and S. Nakanishi. Molecular cloning and characterization of the rat NMDA receptor. *Nature (Lond.)* 354:31–37 (1991).
3. Meguro, H., H. Mori, K. Araki, E. Kushiya, T. Kutsuwada, M. Yamazaki, T. Kumanishi, M. Arakawa, K. Sakimura, and M. Mishina. Functional characterization of a heteromeric NMDA receptor channel expressed from cloned cDNAs. *Nature (Lond.)* 357:70–74 (1992).
4. Monyer, H., R. Sprengel, R. Schoepfer, A. Herb, M. Higuchi, H. Lomeli, N. Burnashev, B. Sakmann, and P. H. Seeburg. Heteromeric NMDA receptors: molecular and functional distinction of subtypes. *Science (Washington D. C.)* 256:1217–1221 (1992).
5. Kutsuwada, T., N. Kashiwabuchi, H. Mori, K. Sakimura, E. Kushiya, K. Araki, H. Meguro, H. Masaki, T. Kumanishi, M. Arakawa, and M. Mishina. Molecular diversity of NMDA receptor channel. *Nature (Lond.)* 358:36–42 (1992).
6. Hollman, M., A. O'Shea-Greenfield, S. W. Rogers, and S. Heinemann. Cloning by functional expression of a member of the glutamate receptor family. *Nature (Lond.)* 342:643–648 (1989).
7. Keinänen, K., W. Wisden, B. Sommer, P. Werner, A. Herb, T. A. Verdoorn, B. Sakmann, and P. H. Seeburg. A family of AMPA-selective glutamate receptors. *Science (Washington D. C.)* 249:556–560 (1990).
8. Boulter, J., M. Hollman, A. O'Shea-Greenfield, M. Hartley, E. Deneris, C. Maron, and S. Heinemann. Molecular cloning and functional expression of glutamate receptor subunit genes. *Science (Washington D. C.)* 249:1033–1037 (1990).
9. Sommer, B., K. Keinänen, T. A. Verdoorn, W. Wisden, N. Burnashev, A. Herb, M. Kohler, T. Takagi, B. Sakmann, and P. H. Seeburg. Flip and flop: a cell-specific functional switch in glutamate-operated channels of the CNS. *Science (Washington D. C.)* 249:1580–1585 (1990).
10. Nakanishi, N., N. A. Shneider, and R. Axel. A family of glutamate receptor genes: evidence for the formation of heteromultimeric receptors with distinct channel properties. *Neuron* 5:569–581 (1990).
11. Sakimura, K., H. Bujo, E. Kushiya, K. Arake, M. Yamazaki, M. Yamazaki, H. Meguro, A. Warashina, S. Numa, and M. Mishina. Functional expression from cloned cDNAs of glutamate receptor species responsive to kainate and quisqualate. *FEBS Lett.* 272:73–80 (1990).
12. Bettler, B., J. Boulter, I. Hermans-Borgmeyer, A. O'Shea-Greenfield, E. S. Deneris, C. Moll, U. Borgmeyer, M. Hollman, and S. Heinemann. Cloning of a novel glutamate receptor subunit, GluR-5: expression in the nervous system during development. *Neuron* 5:583–595 (1990).
13. Werner, P., M. Voigt, K. Keinänen, W. Wisden, and P. H. Seeburg. Cloning of a putative high-affinity kainate receptor expressed predominantly in hippocampal pyramidal cells. *Nature (Lond.)* 351:742–744 (1991).
14. Egebjerg, J., B. Bettler, I. Hermans-Borgmeyer, and S. Heinemann. Cloning of a cDNA for a glutamate receptor subunit activated by kainate but not AMPA. *Nature (Lond.)* 351:745–748 (1991).
15. Sakimura, K., T. Morita, E. Kushiya, and M. Mishina. Primary structure and expression of the $\gamma 2$ subunit of the glutamate receptor channel selective for kainate. *Neuron* 8:267–274 (1992).
16. Sommer, B., N. Burnashev, T. A. Verdoorn, K. Keinänen, B. Sakmann, and P. H. Seeburg. A functional glutamate receptor channel with high affinity for domoate and kainate. *EMBO J.* 11:1651–1656 (1992).
17. Gallo, V., L. M. Upson, W. P. Hayes, L. Vyklicky, C. A. Winters, and A. Buonanno. Molecular cloning and developmental analysis of a new glutamate receptor subunit isoform in cerebellum. *J. Neurosci.* 12:1010–1023 (1992).
18. Kenakin, T. P. *Pharmacologic Analysis of Drug-Receptor Interaction*. Raven Press, New York (1988).
19. Monaghan, D., R. Bridges, and C. Cotman. The excitatory amino acid receptors: their classes, pharmacology and distinct properties in the function of the central nervous system. *Annu. Rev. Pharmacol. Toxicol.* 29:314–320 (1989).
20. Watkins, J. C., P. Krogsgaard-Larsen, and T. Honoré. Structure-activity relationships in the development of excitatory amino acid receptor agonists and competitive antagonists. *Trends Pharmacol. Sci.* 11:25–33 (1990).

21. Verdoorn, T. A., N. W. Kleckner, and R. Dingledine. *N*-Methyl-D-aspartate/kainate receptors expressed in *Xenopus* oocytes: antagonist pharmacology. *Mol. Pharmacol.* **35**:360–368 (1989).
22. Krieg, P. A., and D. A. Melton. Functional messenger RNAs are produced by SP6 *in vitro* transcription of cloned cDNAs. *Nucleic Acids Res.* **12**:7057–7070 (1984).
23. Dawson, T. L., R. A. Nicholas, and R. Dingledine. Homomeric GluR 1 excitatory amino acid receptors expressed in *Xenopus* oocytes. *Mol. Pharmacol.* **38**:779–784 (1990).
24. Ishida, A. T., and J. Neyton. Quisqualate and L-glutamate inhibit retinal horizontal cell responses to kainate. *Proc. Natl. Acad. Sci. USA* **82**:1837–1841 (1985).
25. Kiskin, N. I., O. A. Krishtal, and A. Y. Tsyndrenko. Excitatory amino acid receptors in hippocampal neurons: kainate fails to desensitize them. *Neurosci. Lett.* **63**:225–230 (1986).
26. Zorumski, C. F., and J. Yang. AMPA, kainate and quisqualate activate a common receptor-channel complex on embryonic chick motoneurons. *J. Neurosci.* **8**:4277–4286 (1988).
27. Perouansky, M., and R. Grantyn. Separation of quisqualate- and kainate-selective glutamate receptors in cultured neurons from the rat superior colliculus. *J. Neurosci.* **9**:70–80 (1989).
28. Kiskin, N. I., O. A. Krishtal, and A. Y. Tsyndrenko. Cross-desensitization reveals pharmacological specificity of excitatory amino acid receptors in isolated hippocampal neurons. *Eur. J. Neurosci.* **2**:461–470 (1990).
29. Tse, F. W., S. Weiss, and B. A. MacVicar. Quisqualate agonists occlude kainate-induced current in cultured striatal neurons. *Neuroscience* **43**:429–436 (1991).
30. Patneau, D. K., and M. L. Mayer. Kinetic analysis of interactions between kainate and AMPA: evidence for activation of a single receptor in mouse hippocampal neurons. *Neuron* **6**:785–798 (1991).
31. Hollmann, M., M. Hartley, and S. Heinemann. Ca^{2+} permeability of KA-AMPA-gated glutamate receptor channels depends on subunit combination. *Science (Washington D. C.)* **252**:851–853 (1991).
32. Hume, R., R. Dingledine, and S. Heinemann. Identification of a site in glutamate receptor subunits that controls calcium permeability. *Science (Washington D. C.)* **253**:1028–1031 (1991).
33. Sheardown, M. J., E. O. Nielsen, A. J. Hansen, P. Jacobsen, and T. Honoré. 2,3-Dihydroxy-6-nitro-7-sulfamoyl-benzo(f)quinoxaline: a neuroprotectant for cerebral ischemia. *Science (Washington D. C.)* **247**:571–574 (1990).
34. Patneau, D. K., and M. L. Mayer. Structure-activity relationships for amino acid transmitter candidates acting at *N*-methyl-D-aspartate and quisqualate receptors. *J. Neurosci.* **10**:2385–2399 (1990).
35. Thio, L. L., D. B. Clifford, and C. F. Zorumski. Characterization of quisqualate receptor desensitization in cultured rat hippocampal neurons. *J. Neurosci.* **11**:3430–3441 (1991).
36. Verdoorn, T. A., N. Burnashev, P. Jonns, P. H. Seeburg, and B. Sakmann. Comparisons between the functional properties of glutamate receptors native to CA3 hippocampal neurons and recombinant glutamate receptors.
37. Monyer, H., P. H. Seeburg, and W. Wisden. Glutamate-operated channels: developmentally early and mature forms arise by alternative splicing. *Neuron* **6**:799–810 (1991).
38. Priestly, T., G. N. Woodruff, and J. A. Kemp. Antagonism of responses to excitatory amino acids on rat cortical neurones by the spider toxin argitoxin₈₃₆. *Br. J. Pharmacol.* **97**:1315–1323 (1989).
39. Jonas, P., and B. Sakmann. Functional properties of glutamate receptor channels in isolated patches from CA1 and CA3 pyramidal cells of rat hippocampal slices. *J. Physiol. (Lond.)* **438**:321P (1991).
40. Verdoorn, T. A., and R. Dingledine. Excitatory amino acid receptors expressed in *Xenopus* oocytes: agonist pharmacology. *Mol. Pharmacol.* **34**:298–307 (1988).
41. Randle, J. C. R., T. Guet, A. Cordi, and J. M. Lepagnol. Competitive inhibition by NBQX of kainate/AMPA receptor current and excitatory synaptic potentials: importance of 6-nitro substitution. *Eur. J. Pharmacol.* **215**:237–244 (1992).
42. Huettner, J. E. Glutamate receptor channels in rat DRG neurons: activation by kainate and quisqualate and blockade of desensitization by Con A. *Neuron* **5**:255–266 (1990).

Send reprint requests to: Todd A. Verdoorn, Department of Pharmacology, Vanderbilt University, Nashville, TN 37232–6600.
